Journal of Applied Sciences

ISSN 1812-5654

science alert

ANSInet
an open access publisher
http://ansinet.com

Journal of Applied Sciences 13 (21): 4363-4370, 2013
ISSN 1812-5654 / DOI: 10.3923/jas.2013.4363.4370

Improving SAFT Imaging Technology for Ultrasonic Detection of Concrete Structures

Hengchang Jing
College of Management, Henan University of Science and Technology,
Luoyang, 471003, China

Abstract: Concrete structures were used in civil engineering wildly. In ultrasonic test for concrete structures, B-scan was a preliminary method to display the results of concrete detection which could give a original, poor resolution graphic display of the inner structure because of some kinds of disturbing noise by low-frequency detection. Synthetic Aperture Focusing Technique (SAFT) was one of effect methods in the area, however, when B-scan data were processed by SAFT, wavepacket would be further elongated because low-frequency detection signal covers a relative long period. Therefore, Wavepacket Decomposition Technique (WDT), which could use a few parameters to describe the original signal so that it could avoid the processing of the whole time history of signals, was introduced here to solve this problem. Better focusing effect could be achieved and imaging resolution could be enhanced by combining SAFT with WDT. Numerical simulation and experimental results have proved the efficiency of the technology. Imaging resolution is improved obviously and the embedded object in a test specimen is located accurately.

Key words: Ultrasonic detection, concrete structures, SAFT, WDT, imaging resolution

INTRODUCTION

Due to the important role reinforced concrete elements play in the structures such as buildings, bridges and other infrastructures, Non-Destructive Testing (NDT) and health monitoring during its whole life-cycle need to be considered (Aggelis *et al*., 2011; Wu and Chang, 2006). Usually, two methods are applied to test of concrete structures. One is Ground Penetrating Radar (GPR). Intensely scatter of electromagnetic wave from the reinforced bar results in badly effect for detection of inner objects of concrete structures. The other is ultrasonic test. Because of ultrasonic diffraction, scattering of ultrasonic wave from the reinforced bar is quietly weak compared to the former method. Furthermore, its sensitivity to the abnormity in the continuous medium is high. It is a promising method (Li *et al*., 2005; Chaix *et al*., 2003). But some challenges appear when it comes to real engineering application. Because hardened concrete is a strongly scattering medium with porosity and inhomogenous, several kinds of scattering sources, such as steel bar and coarse or fine aggregates, which are the essential parts of the concrete structures themselves, can cause real problems in the detection (Prassianakis and Prassianakis, 2004; Schickert, 2002; Li *et al*., 2012). To resolve this problem, Synthetic Aperture Focusing Technique (SAFT) is first introduced here to enhance the Signal-to-Noise Ratio (SNR) and improve the reconstructed image's resolution through rough B-scan method (Sun and Shen, 1992; De La Haza *et al*., 2013; Shao *et al*., 2011). This algorithm derives from the imaging technique of Synthetic Aperture Radar (SAR) and the imaging theory of SAFT is explained in next section.

IMAGING THEORY OF SAFT

The SAFT algorithm focuses the received signals to any point of the reconstructed image by coherent superposition (Shao *et al*., 2011; Antonio and Hirose, 2012). In this way, a large virtual transducer with variable focus is synthesized and the schematic diagram of SAFT imaging is showed in Fig. 1.

Because of angle of divergence of ultrasonic transducers, each reflective point inside concrete structure can be detected by transducers on different apertures. In Fig. 1, for example, P (x_i,y_j) is a random reflective point and the vertical distance from P to the scanning line is $R = y_j$. P begins to enter into the detecting area while transducer is placed at position A and P is closest to transducer while the transducer is moved to position O and when the transducer is moved to position B, P leaves the area gradually. If the aperture number between A and B is M, the reflection of P occurs in the mth aperture at distance r_m:

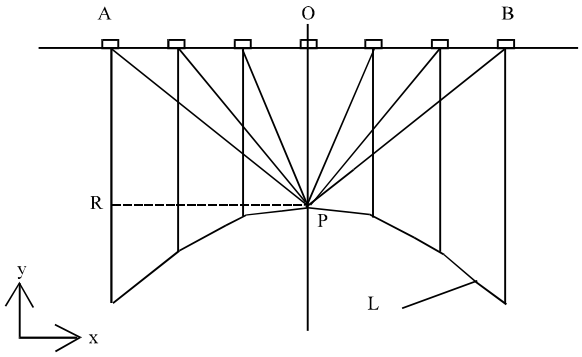

Fig. 1: Schematic diagram of SAFT imaging

$$r_m = \sqrt{R^2 + d_m^2}, \quad m = 1, 2, ..., M \tag{1}$$

where, R is fix value, d_m is the transverse distance from each aperture to P and r_m is expressed as a curve L in Fig. 1. The time of flight (TOF) t_m of reflected echo in each aperture signal is expressed as:

$$t_m = 2r_m/V, \quad m = 1, 2, ..., M \tag{2}$$

where, V represents the average velocity of ultrasound propagating in concrete. In fact, SAFT algorithm aims to highlight P through superposition and average of reflected echo from P in each measured aperture. To the mth aperture measured signal F (d_m,t), the reconstructed process for P can be expressed as Eq. 3:

$$S(x_i, y_i) = \frac{1}{M}\sum_{m=1}^{M} F(d_m, t_m) \tag{3}$$

where, F (d_m, t_m) denotes the echo from P in the mth aperture, S (x_i, y_j) is also called the reconstructed pixel.

APPLICATION OF WDT

Analyse of wavepacket distortion: When ultrasound is propagating in concrete, attenuation of ultrasonic power is big and ultrasonic amplitude is decreased as the exponential times with frequency increasing (Delsanto and Hirsekorn, 2004; Algernon *et al.*, 2008) and then the detecting frequency is usually selected range from 50-500 kHz. The low-frequency ultrasonic signals have advantages, such as strong diffraction, small attenuation, good penetrability and ensuring resolution and so on. In simulation, input signal is adopted as following Eq:

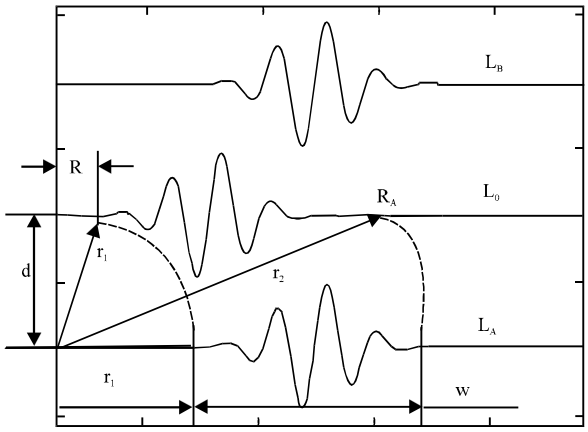

Fig. 2: Sketch of SAFT algorithm

$$h(t) = \cos(2\pi ft) \cdot e^{(-((t-t_p)\cdot w)^2)} \tag{4}$$

It is a cosine wave modulated by gauss function, f is master frequency of the signal and w is the coefficient of pulse width of gauss wave and t_p is the central time of each wavepacket.

According to the principle of ultrasonic propagation, the reflected waveform should conform with input waveform in continuous medium and then the received signals can be described by input signal during processing measured signals (Abbate *et al.*, 1995; Shi *et al.*, 2001). However, wavepackets will be elongated in SAFT because its computational unit is the sampling point and not a whole packet. Three kinds of apertures signals for the same reflective target are showed in Fig. 2. The interval of apertures is d, L_0 is central aperture signal and L_A and L_B are adjacent bilateral apertures signals. Because L_A and L_B have similar condition, wavepacket distortion will be illuminated by taking L_A as an example.

The reflected wavepacket from reflective point begins to appear at position R of L_0 while the distance from reflective point to scanning line is R. Similarly, the reflected wavepacket should begin to appear at position $r_1 = \sqrt{d^2 + R^2}$ of L_A. Their wavepacket width w conforms to input wavepacket. In the light of SAFT algorithm, L_0 is fixed and L_A is adjusted point by point. For L_A, the head point of wavepacket is moved to position R which is the same as the head point of wavepacket in L_0 and then the end point of wavepacket is adjusted to position R_A which can be calculated according to Eq. 5:

$$R_A = \sqrt{r_2^2 - d^2} \tag{5}$$

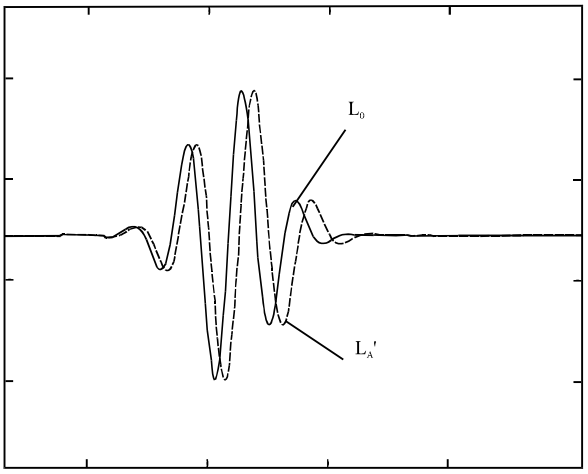

Fig. 3: Sketch of wavepacket distortion

where, r_2=w+r_1. Then the width of wavepacket is changed to w':

$$w' = R_A\text{-}R > w \quad (6)$$

L_A is elongated to L_A' as shown in Fig. 3. It can be seen that almost all points lag behind L_0 except for the head point. SAFT can not reach its best effect because L_0 and L_A' does not fit point by point. Furthermore, the farther the distance from aperture to centre is, the greater wavepacket distortion is. Therefore, WDT is introduced here to solve this problem. Next section will explain the theory and application of WDT.

Theory and application of WDT: The basic idea of WDT is that the input wavepacket is the basic unit to describe test signals. A combination of input wavepacket at different position and with different amplitude can approximate to the test signals (Saenger *et al*., 2011). If input signal is as mother wavepacket and then the measured signals can be as a combination with different time-delay, scale and magnitude mother wavepacket, which can be expressed as Eq. 7:

$$x(t) = \sum_{i=1}^{M} a_i h_i(t) + e(t), i = 1, 2, \ldots M \quad (7)$$

where, e (t) is the approximate errors, h_i (t) is the ith basic wavepacket and a_i is the corresponding amplitude coefficient. The number M of decomposed wavepacket can be decided by approximate requirement and the essential features of signals can be summarized using only a limited number of parameters. The technology is called WDT because this modeling process is similar to

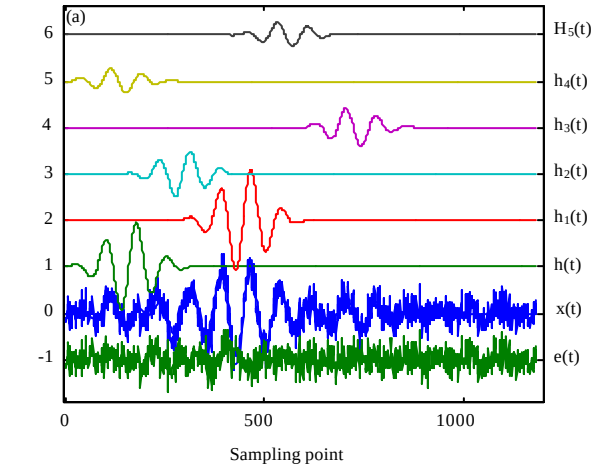

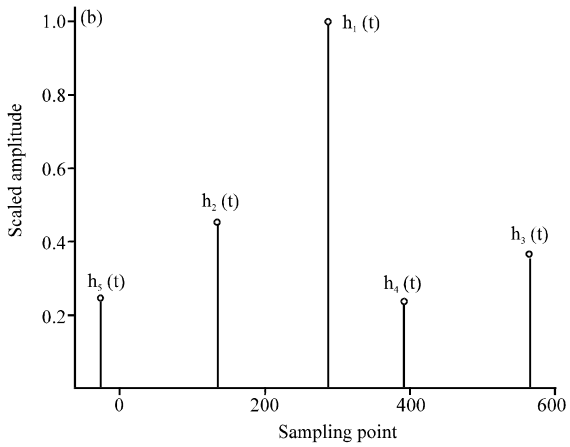

Fig. 4(a-b): Theory of WDT, (a) Sketch of WDT and (b) Distribution of amplitude and location of wavepackets

decompose the signal into several basic wavepackets. Each unit decomposed by WDT is equivalent to the wavepacket that passes through different path and represents the feature of the local region. WDT also has the ability to distinguish the overlapped wavepackets.

If h (t) is selected as input signal, WDT describes the structures of the measured signal by the shifted and attenuated input. Figure 4a is an example result of WDT, where x (t) is a measured signal and it is decomposed into five basic wavepackets denoted by h_1 (t)~h_5 (t). The structure of the original signal can be described by distribution arrival time t_i of and a_i shown in Fig. 4b. Form of each basic wavepacket, which is expressed as Eq. 8, is closed to mother wavepacket except for amplitude and arrival time:

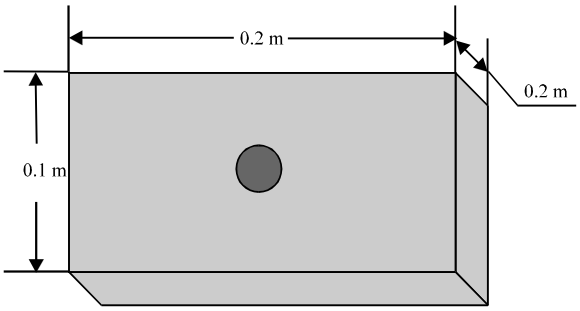

Fig. 5: Single object model of concrete

$$h_i(t) = \cos(2\pi f(t - t_i)) \cdot e^{(-((t-t_p-t_i)\cdot\omega)^2)} \quad (8)$$

where, t_i is arrival time from input wavepacket. So x (t) can be approximated by x'(t) as Eq. 9 which composes of the decomposed wavepackets:

$$x'(t) = \sum_{i=1}^{5} a_i \cdot h_i(t) \approx x(t) \quad (9)$$

WDT is used as a pre-processing method for SAFT. Then, the arrival time t_i are adjusted according to SAFT algorithm, which is equivalent to point-by-point adjusting of the whole wavepacket and the elongation effect mentioned in upper section can be avoided. This new approach can both improve the SAFT focus effect and simplified the focus algorithm. In addition, a great number of disturbing noise is deleted by omitting e (t) and then the Signal-to-Noise Rate (SNR) and resolution of image are further improved.

SIMULATION TO CONCRETE IMAGING

To verify the proposed imaging approach, commercial software WAVE3000, which is a professional simulation software in ultrasonic test, is adopted to simulate ultrasonic detection. Two concrete models are designed for simulation. Two ultrasonic transducers with diameter of 20 mm are used as transmitter and receiver. B-scan data is simulated for the model. h (t) is chosen as input signal and its central frequency is 100 kHz. Four lateral sides are set as infinite.

Single-object detection: The volume of single-object model is (0.2×0.2×0.1 m). A steel cylinder as inside detected object is placed at centre of model which is showed in Fig. 5.

B-scan is achieved along the linear aperture of model upper surface and image by original received signals is quite rough as showed in Fig. 6a. Figure 6b is the processed image with direct SAFT and after adding WDT, the processed image is as showed in Fig. 6c. By comparison, focusing effect is more obvious and the resolution is improved after adding WDT. In Fig. 6c, bulge

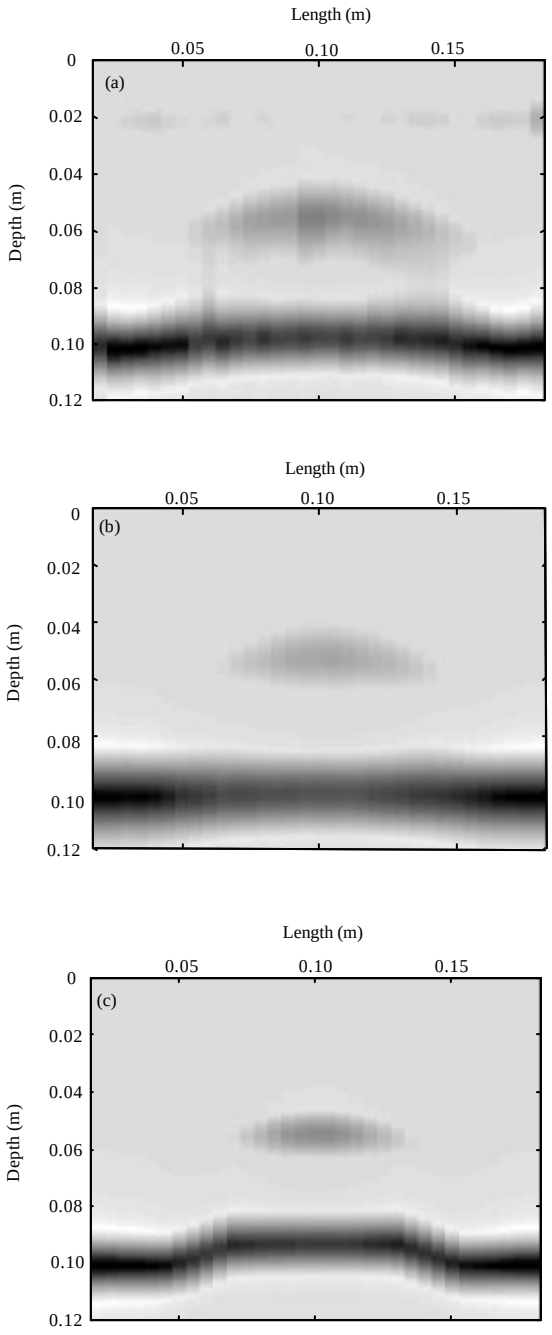

Fig. 6(a-c): Simulation for single object (a) Original image, (b) Image of SAFT before introducing WDT, (c) Image of SAFT after introducing WDT

of bottom below the steel cylinder can owe to the second echo from the cylinder where the ultrasonic wave cannot reach the bottom of model, thus the partly bottom is alike to be elevated. In Fig. 6b, however, because wavepacket distortion results in inaccurate focusing, the second echo is blurred and cannot be seen.

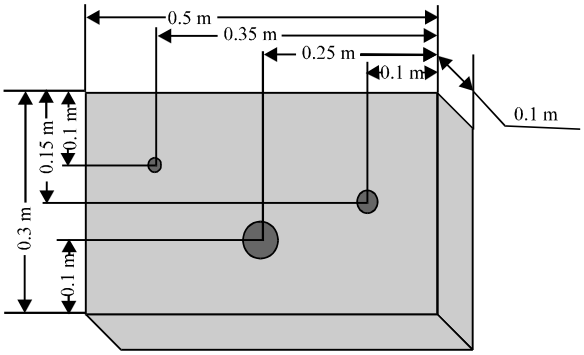

Fig. 7: Three objects model of concrete

Three-objects detection: The volume of three-object model is (0.5×0.1×0.3 m). Three cylinders, diameters are 20, 50, 30 mm, respectively, which are as detected objects are placed into the model, as showed in Fig. 7.

To embody ability of WDT in the matter of removing noise, a number of random noise is added in detecting signals and the original image is mapped in Fig. 8a. From the Figure, the reflected curse from the objects is submerged and hard to be identified. Figure 8b is the process ed image with direct SAFT and after adding WDT, the processed image is as showed in Fig. 8c. By comparison, before adding WDT, focusing effect is terrible and the embedded objects are unobvious because of the random noise. After introducing WDT, however, not only is the random noise removed but also focusing effect is more obvious and the resolution is improved and the embedded objects are clear.

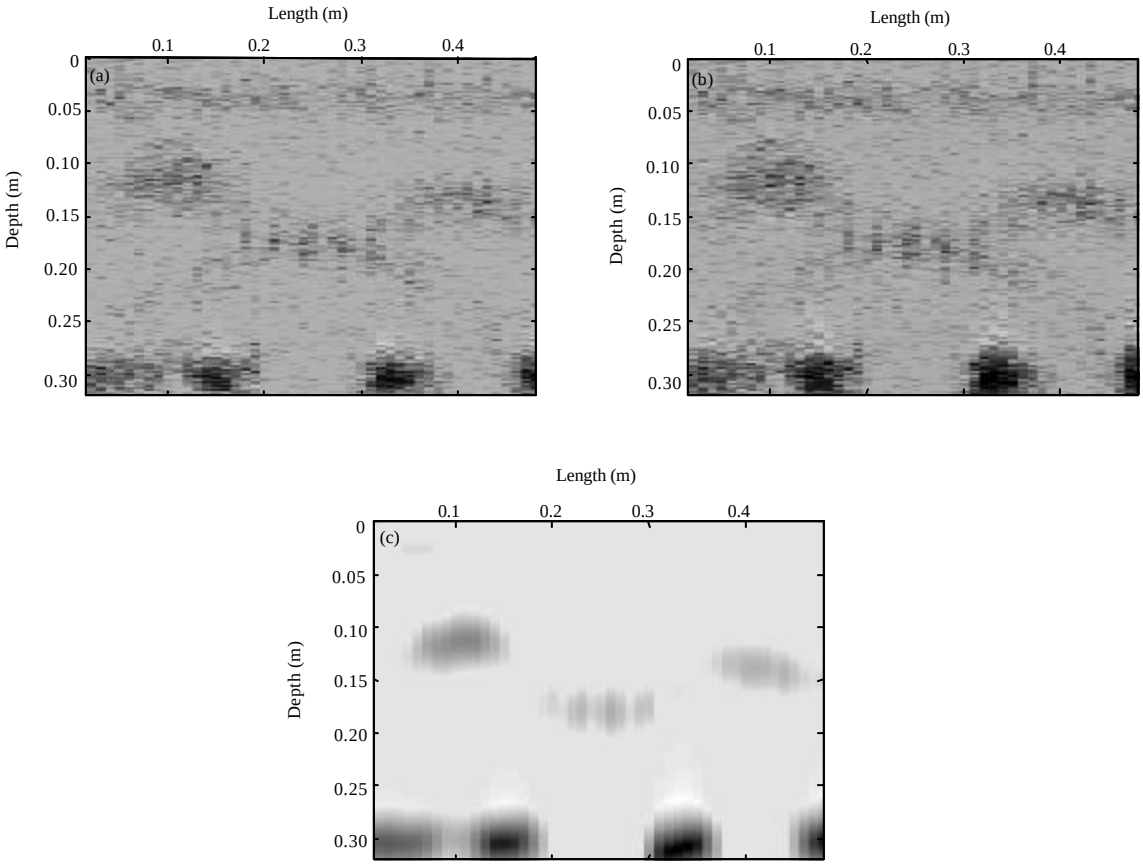

Fig. 8(a-c): Simulation of three objects (a) Original image, (b) Image of SAFT before introducing WDT and (c) Image of SAFT after introducing WDT

EXPERIMENTAL RESEARCHES

Although, it has been verified that the proposed method is effective from the upper numerical simulation, the simulation which has certain limitation still can not replace the practical processes and results. Therefore, a detection experiment is conducted on a concrete specimen in order to further verify the method.

Experimental system: A detection system is established as Fig. 9 and a concrete specimen is cast as the normal architectural concrete and its dimensions are of (500×300×200) mm^3. A steel pipe with diameter of 50 mm is embedded in as shown in Fig. 10. h (t) is still chosen as input signal and its central frequency is 50 kHz. A pair of market available 50 kHz ultrasonic transducers made from KCRT Company are selected and the diameters of them are all 40 mm. One is used as transmitter and the other is used as receiver in B-scan experiment.

Velocity measurement: The ultrasonic velocity in specimen needs to be measured before imaging. Measurement of velocity is conducted at the left section of the specimen. Firstly, the velocity is measured by ultrasonic penetration testing which is widely used in engineering and its result is closer to real values. After the measurement in several positions on the specimen, the average velocity is obtained as 4255.3 m sec^{-1}. However, sometimes there is only one plane in concrete detection, so the pulse-echo test on single plane is adopted and its result is compared with the penetration testing.

The transmitter is coupled with glycerin and positioned on the one side of surface of specimen away from the PVC pipe and the receiver is located at the other position and the distance between two transducers is set as 50 mm (the distance is the length between centers of two transducers, which is determined by outside diameter of the transducers) as shown in Fig. 11. By moving the receiver at the step of 20 mm, reflected waveforms from backwall are collected on six positions, respectively.

The reflected waves can be extracted by WDT and their TOF t_i can be calculated. Then velocity on each point and average velocity of ultrasound can be calculated according to Eq. 10. The results are listed in Table 1:

$$v = \sqrt{\frac{(d_{i+1}^2 - d_i^2)}{(t_{i+1}^2 - t_i^2)}},\ i = 1,2,...5 \qquad (10)$$

Here d_{i+1} and d_i are the distance of two transducers, respectively, t_{i+1} and t_i are the corresponding TOF. Table 1 shows the measured result of pulse-echo method is very close to the result of penetration testing.

Table 1: Velocity calculated from adjacent measurement points

Distance of center (mm)	Velocity (m sec^{-1})
50	/
70	4170.7
90	4012.1
110	4072.3
130	4259.6
150	4254.0
Average	4166.7

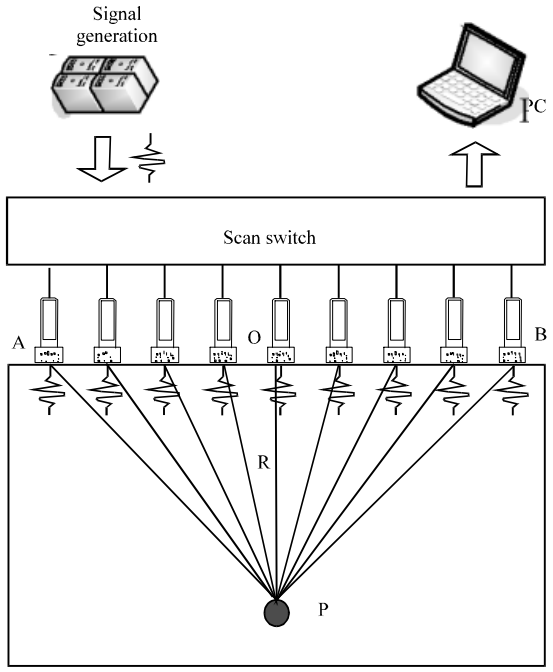

Fig. 9: Sketch-map of a B-scan system

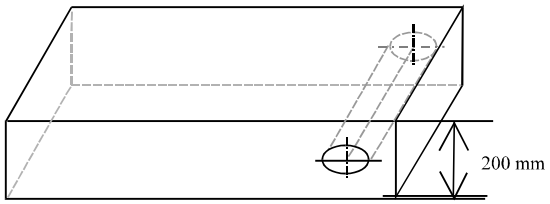

Fig. 10: Structure of concrete specimen

Imaging results: An imaging experiment of B-scan along the length direction of specimen is carried out after velocity measurement. The results are shown in Fig. 12. In the figure, the dashed straight line represents the position of backwall and the dashed circle shows the position of PVC pipe in the specimen. It can be seen clearly that the echoes from the pipe which are submerged in surface waves are not able to be inspected in its position. Figure 12 is only a direct imaging of B-scan data which has limited resolution and there still exist some disturbing signals in the image.

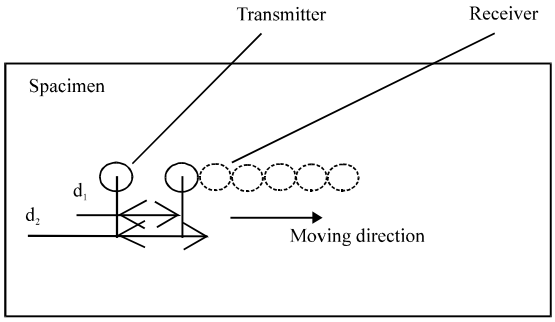

Fig. 11: Method of single-side measurement

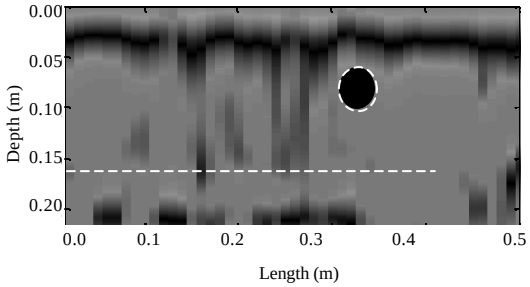

Fig. 12: B-scan imaging results

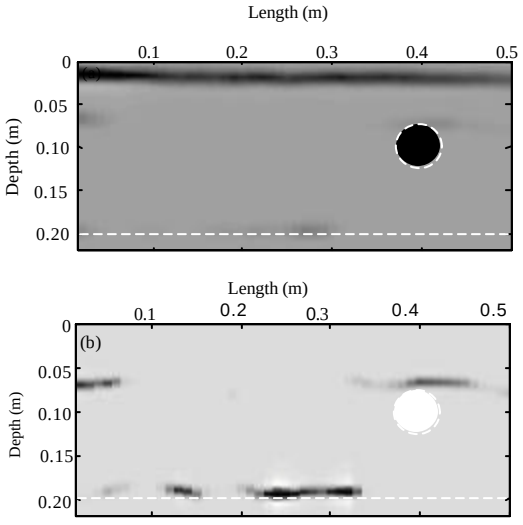

Fig. 13: SAFT imaging results

Figure 13 gives the focusing results by SAFT. Figure 13a is the processing result by SAFT and Fig. 13b is the processing result by WDT improved SAFT. From Fig. 13a, focusing effect is poor and the echoes are not clear because of wavepacket distortion, and furthermore the echoes from the pipe and backwall are so weak because of high energy of surface wave. After using WDT, the surface waves can be identified as the first wavpacket and removed, then the rest part of data are processed by improved SAFT. The final imaging result is displayed in Fig. 13b. Compared to the image in Fig. 13a, it can be seen that the echoes from the pipe and backwall are highlighted after removing the surface wave and more clear image is obtained because noise is also omitted. The positions of the pipe and backwall shift a little upward because the estimated wave velocity is a little smaller than the real one. Two black strips on both sides may be the reflection from the boundaries of specimen. It can be avoided when the transducers are kept at certain distance from the boundaries.

CONCLUSION

SAFT is an effective method to improve imaging resolution in low frequency ultrasonic test of concrete structures. Because of wavepacket distortion and disturbing noise, focusing effect is reduced. Therefore WDT is introduced to improve SAFT algorithm and then the SNR and resolution of image is improved and calculation of SAFT is cut down greatly. From the results of simulation, focusing effect is more obvious and resolution is higher. This proposed method provides an effective processing way for high resolution test.

ACKNOWLEDGMENTS

This study was supported by National Natural Science Foundation of China (11264032).

REFERENCES

Abbate, A., J. Frankel and P. Das, 1995. Wavelet transform signal processing for dispersion analysis of ultrasonic signals. Proceedings of the IEEE Ultrasonics Symposium, November 7-10, 1995, Seattle, WA., pp: 751-755.

Aggelis, D.G., E.Z. Kordatos, M. Strantza, D.V. Soulioti and T.E. Matikas, 2011. NDT approach for characterization of subsurface cracks in concrete. Constr. Build. Mater., 25: 3089-3097.

Algernon, D., B. Grafe, F. Mielentz, B. Kohler and F. Schubert, 2008. Imaging of the elastic wave propagation in concrete using scanning techniques: Application for impact-echo and ultrasonic echo methods. J. Nondestructive Evaluation, 27: 83-97.

Antonio Jr. O.V.M. and S. Hirose, 2012. Ultrasonic imaging of concrete by synthetic aperture focusing technique based on hilbert-huang transform of time domain data. Mater. Trans., 53: 621-626.

Chaix, J.F., V. Garnier and G. Corneloup, 2003. Concrete damage evolution analysis by backscattered ultrasonic waves. NDT&E Int., 36: 461-469.

De la Haza, A.O., A.A. Samokrutov and P.A. Samokrutov, 2013. Assessment of concrete structures using the Mira and Eyecon ultrasonic shear wave devices and the SAFT-C image reconstruction technique. Constr. Build. Mater., 38: 1276-1291.

Delsanto, P.P. and S. Hirsekorn, 2004. A unified treatment of nonclassical nonlinear effects in the propagation of ultrasound in heterogeneous media. Ultrasonics, 42: 1005-1010.

Li, Q.F., P. Huang and Y. Liao, 2012. Research on SAFT imaging method of array probes in concrete structures. Applied Mech. Mater., 189: 265-269.

Li, Z.Q., F. Xi and Z.H. Shui, 2005. Comparison of radar and ultrasonic CT images in Non-destructive testing. J. Huazhong Univ. Sci. Technol., 22: 1-3.

Prassianakis, I.N. and N.I. Prassianakis, 2004. Ultrasonic testing of Non-metallic materials: Concrete and marble. Theor. Applied Fracture Mech., 42: 191-198.

Saenger, E.H., G.K. Kocur, R. Jud and M. Torrilhon, 2011. Application of time reverse modeling on ultrasonic non-destructive testing of concrete. Applied Math. Modell., 35: 807-816.

Schickert, M., 2002. Ultrasonic NDE of concrete. Proceedings of the IEEE Ultrasonics Symposium, Volume 1, October 8-11, 2002, Institute of Electrical and Electronics Engineers, New York, pp: 718-727.

Shao, Z., L. Shi, Z. Shao and J. Cai, 2011. Design and application of a small size SAFT imaging system for concrete structure. Rev. Scient. Instrum., 82: 1-9.

Shi, L., B. Chen, C. Gao and B. Zhou, 2001. Design and modeling of signals by using wavelets for the Pulse-echo NDT Approaches. Proc. SPIE, 4336: 146-153.

Sun, B.S. and J.Z. Shen, 1992. Synthetic aperture focusing ultrasonic imaging (1). Applied Acoustics, 12: 43-48.

Wu, F. and F.K. Chang, 2006. Debond detection using embedded piezoelectric elements in reinforced concrete structures-Part I: Experiment. Structural Health Monit., 5: 5-15.